Proceedings of the 12th Workshop on Quantum Chaos and Localisation Phenomena (CHAOS 25)

An Idea for Measuring Spatial Coherency Matrices by Multiplexing Across a Reconfigurable Complex System onto a Single-Port Intensity Detector

P. del Hougne*

Univ Rennes, CNRS, IETR — UMR 6164, F-35000 Rennes, France

Doi: 10.12693/APhysPolA.148.S39 *e-mail: philipp.del-hougne@univ-rennes.fr

We propose a technique for measuring the spatial coherency matrix of a wavefront based on a single-port intensity detector. Our method relies on multiplexing the incident wavefront across a series of known realizations of a reconfigurable complex system onto the intensity detector. We consider a multi-port chaotic cavity with partially reconfigurable boundary conditions as an embodiment of the reconfigurable complex system. This matches recent experiments with 3D chaotic cavities whose walls are partially covered with a programmable metasurface. We formulate a system model that rigorously accounts for multiple scattering based on multi-port network theory. Then, we numerically validate the principle. The appeal of our technique lies in the low hardware complexity.

topics: coherency matrix, multiplexing, programmable metasurface, single-pixel camera

1. Introduction

The characterization of the second-order statistics of a wavefront via its spatial coherency matrix is of great importance across the electromagnetic spectrum, with diverse applications in encryption, communication, and sensing. A direct measurement of the coherency matrix of an N-channel wavefront requires N phase-coherent, simultaneously sampled receiver chains synchronized to a common time and frequency reference, followed by computations of all second-order products from the time traces, i.e., N powers and $\binom{N}{2}$ complex cross-correlations. The required hardware for such direct measurements scales poorly; alternative techniques to measure the coherency matrix for large N or high frequencies are hence desirable.

In the optical frequencies range, a number of indirect techniques for measuring the coherency matrix have been developed. They are typically of a tomographic nature, projecting the wavefront across a system onto numerous intensity detectors. The utilized system can be a carefully designed [1–10] or a carefully characterized random system [11]. Furthermore, a carefully designed self-configuring system has been shown in theory to be additionally capable of diagonalizing the coherency matrix [12].

To further reduce the detector complexity, operation with a single-port intensity detector is desirable [13, 14]. Here, we propose and analyze such a scheme based on multiplexing the wavefront across configurations of a reconfigurable complex system. Our approach is particularly well-suited to microwave systems where reconfigurable complex systems can be realized based on chaotic cavities equipped with programmable metasurfaces, for which accurate system models can be experimentally calibrated [15–17]. Indeed, our approach is inspired by works on computational microwave imaging, which multiplex scene information across different configurations of a programmable microwave meta-imager [18, 19]. Related ideas have recently been presented also for low-complexity wireless multi-port sensing [20]. Our technique rigorously accounts for all multiple-scattering effects.

The remainder of this paper is organized as follows. In Sect. 2, we formalize our problem statement. In Sect. 3, we describe our method. In Sect. 4, we present a numerical validation of our technique. In Sect. 5, we briefly conclude and discuss directions for future work.

2. Problem statement

2.1. Goal

Our goal is to characterize the second-order statistics of an N-channel wavefront $\boldsymbol{x} \in \mathbb{C}^N$ by estimating its *coherency matrix*

$$\Gamma \triangleq \mathbb{E}\left[\boldsymbol{x}\boldsymbol{x}^\dagger\right] \quad \in \mathbb{C}^{N\times N}, \tag{1}$$

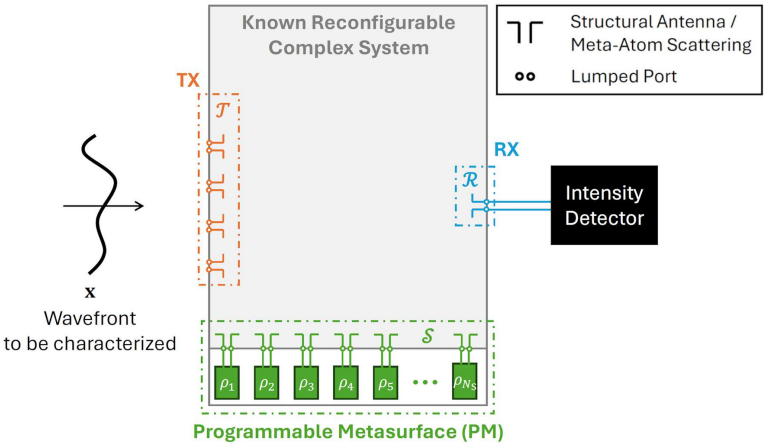

Fig. 1. System model.

which is Hermitian positive semidefinite; here, † denotes the conjugate transpose. More specifically, we aim to estimate Γ based on a single-port intensity detector by multiplexing $\boldsymbol{x}$ across different known realizations of a reconfigurable complex system. We assume that the *statistical* properties of $\boldsymbol{x}$ are time-invariant over the course of all measurements conducted as part of our technique.

2.2. Multiplexing onto a single-port intensity detector

Interactions with scattering systems alter the coherency matrix in a known manner. A linear M-port system characterized by its scattering matrix $S \in \mathbb{C}^{M\times M}$ maps an incoming wavefront $\boldsymbol{a} \in \mathbb{C}^M$ to the corresponding outgoing wavefront

$$\boldsymbol{b} = S\boldsymbol{a} \quad \in \mathbb{C}^M. \tag{2}$$

Let the coherency matrix of the incoming wavefront be $\Gamma_{\text{in}} \triangleq \mathbb{E}\left[\boldsymbol{a}\boldsymbol{a}^\dagger\right]$. Then, assuming negligible thermal emission from the system, the coherency matrix of the outgoing wavefront is given by

$$\Gamma_{\text{out}} \triangleq \mathbb{E}\left[\boldsymbol{b}\boldsymbol{b}^\dagger\right] = \mathbb{E}\left[(S\boldsymbol{a})(S\boldsymbol{a})^\dagger\right] = S\Gamma_{\text{in}}S^\dagger. \tag{3}$$

In our case, $M = N + 1$, because we inject via N input ports and receive via the output port connected to the intensity detector. Let $\mathcal{T}$ and $\mathcal{R}$ denote the sets containing the N input port indices and the output port index, respectively. This leads to a 2×2 partition of S,

$$S = \begin{bmatrix} S_{\mathcal{T}\mathcal{T}} & S_{\mathcal{T}\mathcal{R}} \\ S_{\mathcal{R}\mathcal{T}} & S_{\mathcal{R}\mathcal{R}} \end{bmatrix}. \tag{4}$$

Because the cardinality of $\mathcal{R}$ is unity, the off-diagonal block $S_{\mathcal{R}\mathcal{T}}$ is, in fact, a $1 \times N$ row vector in our case; for clarity, we denote it by $\boldsymbol{t} \triangleq S_{\mathcal{R}\mathcal{T}}$. Without excitation at the output port, i.e., $\boldsymbol{a}_{\mathcal{R}} = \boldsymbol{0}$, the outgoing field at the output port is

$$y = b_{\mathcal{R}} = \boldsymbol{t}\,\boldsymbol{a}_{\mathcal{T}} = \boldsymbol{t}\,\boldsymbol{x}. \tag{5}$$

The output coherency on the receiving side is

$$\gamma' = \boldsymbol{t}\,\Gamma\,\boldsymbol{t}^\dagger \quad \in \mathbb{R}_{\geq 0}, \tag{6}$$

which is a scalar because there is only one output port. Since γ' is an average intensity, it is real and non-negative. Our single-port intensity detector measures

$$I \triangleq \mathbb{E}\left[|y|^2\right] = \gamma'. \tag{7}$$

Of course, a measurement of the scalar γ' does not contain sufficient information to recover the matrix Γ (unless there is additional prior knowledge about Γ). However, we can accumulate sufficient information by measuring γ' for different realizations of $\boldsymbol{t}$. Specifically, let $\boldsymbol{t}_k$ denote the k-th realization of $\boldsymbol{t}$, and let I_k denote the corresponding k-th measurement of I. We can stack our K measurements as follows

$$\boldsymbol{i} \triangleq [I_1, \ldots, I_K]^{\mathrm{T}} \quad \in \mathbb{R}^K,$$
$$H \triangleq \begin{bmatrix} \boldsymbol{t}_1 \\ \vdots \\ \boldsymbol{t}_K \end{bmatrix} \in \mathbb{C}^{K\times N}. \tag{8}$$

The relation between $\boldsymbol{i}$ and H can be compactly summarized as

$$\boldsymbol{i} = \mathrm{diag}\left(H\,\Gamma\,H^\dagger\right), \tag{9}$$

where $\mathrm{diag}(\cdot)$ extracts the vector of diagonal entries. If H is sufficiently diverse, we can hope that $\boldsymbol{i}$ contains sufficient information to recover Γ.

2.3. Multi-port network model of the reconfigurable complex system

We aim to realize K known and diverse realizations of $\boldsymbol{t}$ based on a reconfigurable complex system. Specifically, we consider a chaotic cavity whose boundaries are partially covered by a programmable metasurface. Each programmable meta-element is parametrized by a tunable lumped element (e.g., a

PIN diode). Conceptually, the programmable meta-atom can be thought of as an antenna whose port is terminated by a tunable load. The resulting system model of the reconfigurable complex system is illustrated in Fig. 1. We assume that the system is passive, linear, reciprocal, and time-invariant.

We partition the system into three entities:

(i) the set of $M = N + 1$ accessible ports;

(ii) the N_S tunable elements of the programmable metasurface, each modeled as a lumped "virtual" port terminated by a load with reflection coefficient $\rho_i \in \mathbb{C}$;

(iii) all static scatterers (cavity walls, scattering objects inside the cavity, structural scattering of the antennas and meta-atoms).

For simplicity, we use the same reference impedance $Z_0 = 50\,\Omega$ at all ports and assume that the intensity detector is matched to Z_0.

Entity (iii) is a P-port system characterized by its scattering matrix $\check{S} \in \mathbb{C}^{P\times P}$, where $P = M + N_\mathrm{S}$. Meanwhile, entity (ii) is a N_S-port system characterized by its scattering matrix

$$\Phi_k = \mathrm{diag}\left(\left[\rho_1^{(k)}, \ldots, \rho_{N_\mathrm{S}}^{(k)}\right]\right) \quad \in \mathbb{C}^{N_\mathrm{S}\times N_\mathrm{S}}, \tag{10}$$

where ρ_i denotes the reflection coefficient of the load terminating the i-th "virtual" port associated with the i-th meta-atom. The index k denotes the k-th considered configuration of the programmable metasurface.

The "measurable" M-port scattering matrix at the accessible system ports is given by standard multi-port network theory (accounting for all multiple scattering effects) [21–23], i.e.,

$$S_k = \check{S}_{\mathcal{A}\mathcal{A}} + \check{S}_{\mathcal{A}\mathcal{S}}\big(\Phi_k^{-1} - \check{S}_{\mathcal{S}\mathcal{S}}\big)^{-1}\check{S}_{\mathcal{S}\mathcal{A}} \quad \in \mathbb{C}^{M\times M}, \tag{11}$$

where $\mathcal{A} = \mathcal{T} \cup \mathcal{R}$ and $\mathcal{S}$ denotes the set of "virtual" port indices. It follows that

$$\boldsymbol{t}_k \triangleq \check{S}_{\mathcal{R}\mathcal{T}} + \check{S}_{\mathcal{R}\mathcal{S}}\big(\Phi_k^{-1} - \check{S}_{\mathcal{S}\mathcal{S}}\big)^{-1}\check{S}_{\mathcal{S}\mathcal{T}}. \tag{12}$$

Given $\check{S}$ and Φ_k for all considered realizations of the programmable metasurface, we can construct H based on (12). While $\check{S}$ and Φ_k cannot be estimated unambiguously in experiments, operationally equivalent proxies can be obtained, as recently demonstrated in [15–17].

Remark: For $N_\mathrm{S} = 1$, the differential output signal (i.e., the change in output signal after reconfiguring the tunable element) is "frozen" in a single spatial mode and always perfectly coherent, independent of the input field's spatial coherence [24].

3. Method

We parametrize the sought-after coherency matrix Γ as $\Gamma = BB^\dagger$, where $B \in \mathbb{C}^{N\times N}$, in order to ensure that Γ is Hermitian positive semidefinite. We do *not* assume prior knowledge about other properties of Γ, such as its rank or trace. To estimate Γ, we minimize the mean-squared error between measured and predicted intensities for the K system configurations,

$$\mathcal{L}(B) = \frac{1}{K}\,\|\,\widehat{\boldsymbol{i}}(B) - \boldsymbol{i}\,\|_2^2 + \lambda\|B\|_F^2, \tag{13}$$

where $\widehat{\boldsymbol{i}}(B)$ denotes the prediction of $\boldsymbol{i}$ using our system model for our current estimate of B. The second term on the right-hand side is a small ridge regularizer with $\lambda = 10^{-10}$ for numerical stability.

Before optimization, we apply per-pattern energy normalization. Specifically, for each configuration k, we replace $\boldsymbol{t}_k$ and I_k by $\bar{\boldsymbol{t}}_k = \boldsymbol{t}_k/\tau_k$ and $\bar{I}_k = I_k/\tau_k^2$, where $\tau_k \triangleq \sqrt{\|\,\boldsymbol{t}_k\,\|_2^2 + \varepsilon}$ with $\varepsilon = 10^{-12}$, ensuring numerical stability.

We optimize the entries of B to minimize $\mathcal{L}(B)$ using the Adam optimizer in TensorFlow. We initialize the real and imaginary parts of the entries of B with a truncated normal distribution of zero mean and a standard deviation of 0.1. We clip the gradient norm at 5.0 and run the algorithm for 50000 iterations with a piecewise constant learning-rate schedule (initially 10^{-3}, from the 5000th iteration onward 5×10^{-4}, and from the 10000th iteration onward 10^{-4}). We use all available data and run our algorithm 50 times with different initial seeds, retaining the result from the run that yielded the lowest cost at the end.

4. Numerical validation

4.1. Generation of synthetic data

To test the proposed method numerically, we generate a synthetic realization of $\check{S}$ following [25]. This realization is a draw from an ensemble of statistical realizations of $\check{S}$ which are reciprocal, obey the coherent-backscattering variance rule (diagonal variance twice the off-diagonal variance), and are globally scaled to ensure passivity (spectral norm well below unity). We use the same parameters as [25] with $\kappa = 1$.

We choose $N_\mathrm{S} = 100$ and assume that the programmable meta-atoms are 1-bit programmable with $\rho_i^{(k)} \in \{+1, -1\}$, in line with [25]. We draw the states of each considered configuration randomly.

For concreteness, we choose $N = 4$ and randomly generate the ground-truth Γ to correspond to a partially coherent wavefront. Specifically, we instantiate the partially coherent input as $\Gamma = U\,\mathrm{diag}(1, 0.2)\,U^\dagger + 0.12\,I$ with U being the first two columns of a random unitary (obtained from the QR decomposition of a random complex Gaussian matrix), and a final scaling is applied to enforce $\mathrm{Tr}(\Gamma) = 1$.

We assume that measurement noise is negligible.

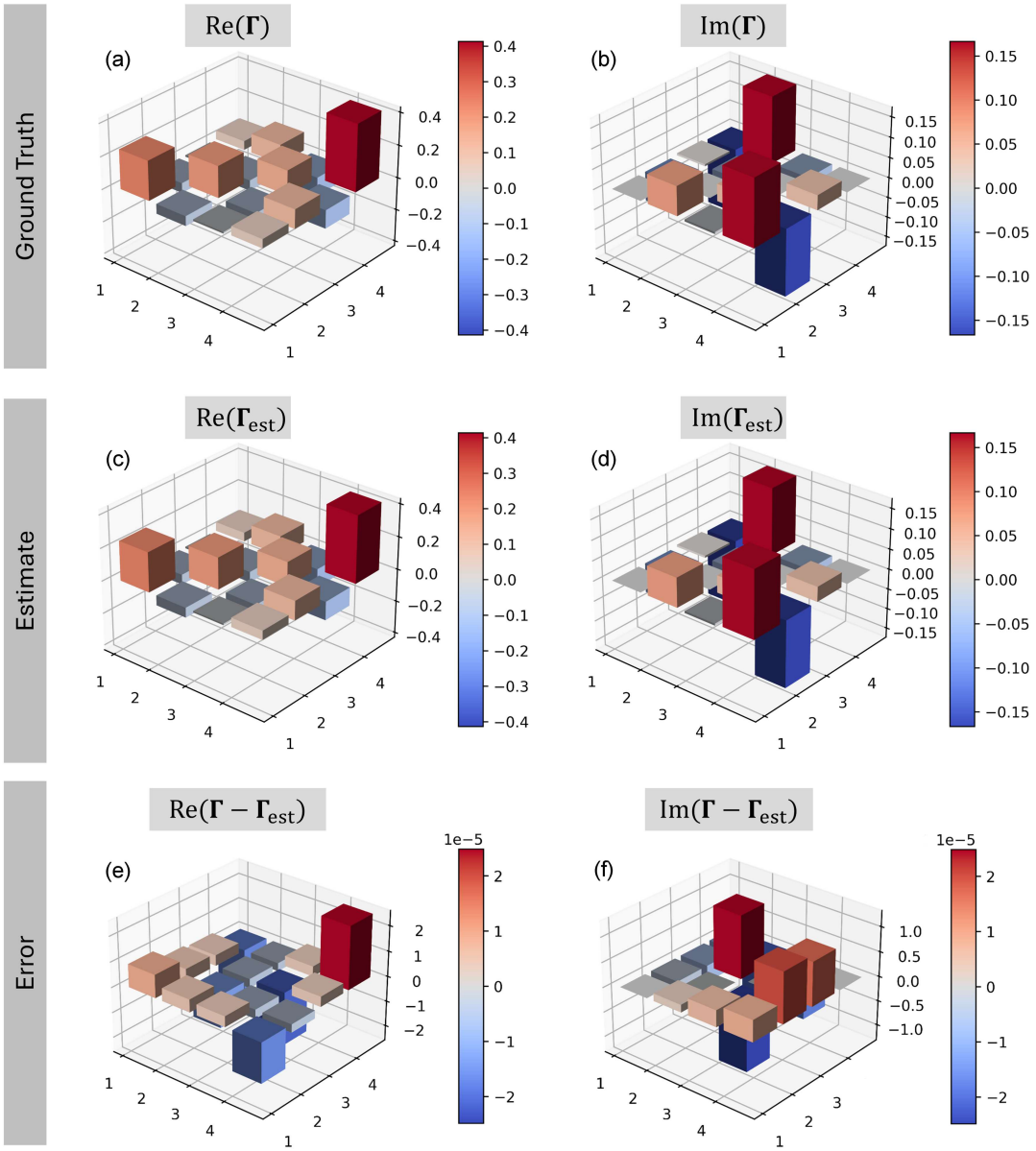

Fig. 2. Ground truth (a, b) and estimate under ideal conditions with $K = 3000$ and without measurement noise (c, d); the error of the estimate is shown in panels (e) and (f). The ideal conditions explain the high accuracy (low error) of the estimate.

4.2. Results

We begin by examining the results of our technique under ideal conditions with a very large number of system configurations $K = 3000$. A representative result is presented in Fig. 2. The flawless estimate of Γ therein validates the principle of the proposed method.

We also examined more systematically how the normalized mean-squared error (NMSE) depends on the number of utilized system configurations, again under noiseless conditions. The result is presented in Fig. 3 and shows a clear threshold for the minimum required value of K of the order of 20. Indeed, the NMSE drastically drops as a function of K around this threshold. This value is of the order of the number of real-valued unknowns in Γ, which is $N^2 = 16$ (because Γ is a Hermitian matrix).

5. Conclusions

5.1. Summary

To summarize, we have proposed and numerically validated a technique for estimating the spatial coherency matrix of a wavefront using a single-port intensity detector, by multiplexing the

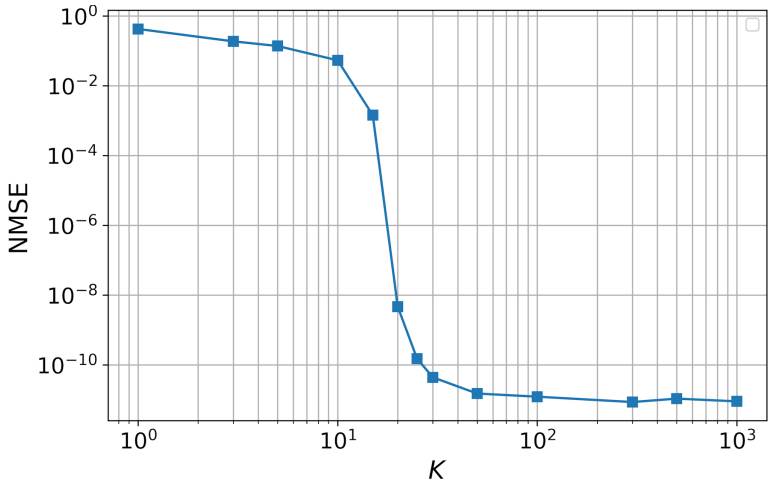

Fig. 3. Dependence of NMSE on K under ideal, noiseless conditions.

wavefront across a series of known realizations of a reconfigurable complex medium. Our numerical evaluation is based on a rigorous multi-port network formulation that fully captures all relevant multiple-scattering events. We have systematically investigated how the number of utilized system realizations influences the estimation accuracy.

5.2. Outlook

Looking ahead, we envision numerous future research directions building on the present work:

- Instead of using a random series of metasurface configurations, the utilized series of configurations can be chosen to optimize relevant properties (such as the diversity) of H [26].
- Prior knowledge about Γ (e.g., about its rank or trace) can be used in an updated version of the algorithm.
- Systematic studies of the estimation accuracy as a function of K and the measurement noise level are needed.
- Experimental validations leveraging (experimentally characterized) reconfigurable complex systems like [15–17] are a promising future research direction. Given the maturity of the hardware and model calibration of such systems at 2.45 GHz [16–17], this frequency regime is very promising for initial experimental tests.

Acknowledgments

This work was supported in part by the ANR France 2030 program (project ANR-22-PEFT-0005) and the ANR PRCI program (project ANR-22-CE93-0010).

References

[1] L. Tian, J. Lee, S.B. Oh, G. Barbastathis, *Opt. Express* **20**, 8296 (2012).

[2] H. Partanen, J. Turunen, J. Tervo, *Opt. Lett.* **39**, 1034 (2014).

[3] B. Stoklasa, L. Motka, J. Rehacek, Z. Hradil, L. L. Sánchez-Soto, *Nat. Commun.* **5**, 3275 (2014).

[4] A.F. Abouraddy, K.H. Kagalwala, B.E. Saleh, *Opt. Lett.* **39**, 2411 (2014).

[5] K.H. Kagalwala, H.E. Kondakci, A.F. Abouraddy, B.E. Saleh, *Sci. Rep.* **5**, 15333 (2015).

[6] K. Saastamoinen, L.-P. Leppänen, I. Vartiainen, A.T. Friberg, T. Setälä, *Optica* **5**, 67 (2018).

[7] Z. Huang, Y. Chen, F. Wang, S.A. Ponomarenko, Y. Cai, *Phys. Rev. Appl.* **13**, 044042 (2020).

[8] Z. Wang, X. Lu, W. Huang, A. Konijnenberg, H. Zhang, C. Zhao, Y. Cai, *Appl. Phys. Lett.* **119**, 111101 (2021).

[9] Y. Zhou, J. Zhao, D. Hay, K. McGonagle, R.W. Boyd, Z. Shi, *Phys. Rev. Lett.* **127**, 040402 (2021).

[10] T. Shirai, A.T. Friberg, *Opt. Lett.* **46**, 4160 (2021).

[11] K. Lee, Y. Park, *Phys. Rev. Appl.* **12**, 024003 (2019).

[12] C. Roques-Carmes, S. Fan, D.A. Miller, *Light Sci. Appl.* **13**, 260 (2024).

[13] J.-P. Liu, C.-H. Guo, W.-J. Hsiao, T.-C. Poon, P. Tsang, *Opt. Lett.* **40**, 2366 (2015).

[14] A.C. Mandal, T. Sarkar, Z. Zalevsky, R.K. Singh, *Sci. Rep.* **12**, 4564 (2022).

[15] J. Sol, H. Prod'homme, L. Le Magoarou, P. del Hougne, *Nat. Commun.* **15**, 2841 (2024).

[16] P. del Hougne, *IEEE Wirel. Commun. Lett. early access*, Nov. 12 (2025).

[17] P. del Hougne, arXiv:2507.22750 (2025).

[18] T. Sleasman, M.F. Imani, J.N. Gollub, D.R. Smith, *Appl. Phys. Lett.* **107**, 204104 (2015).

[19] Y.B. Li, L.L. Li, B.B. Xu, W. Wu, R.Y. Wu, X. Wan, Q. Cheng, T.J. Cui, *Sci. Rep.* **6**, 23731 (2016).

[20] P. del Hougne, arXiv:2509.24537 (2025).

[21] B.D.O. Anderson, R.W. Newcomb, *Proc. Inst. Electr. Eng.* **113**, 970 (1966).

[22] T.T. Ha, *Solid-State Microwave Amplifier Design*, Wiley-Interscience, 1981.

[23] H. Prod'homme, P. del Hougne, arXiv:2412.17884 (2024).

[24] P. del Hougne, arXiv:2509.09506 (2025).

[25] C. Hammami, L. Le Magoarou, P. del Hougne, arXiv:2508.01776 (2025).

[26] P. del Hougne, M. Davy, U. Kuhl, *Phys. Rev. Appl.* **13**, 041004 (2020).